Effect of Coriolis Force on the Shear Viscosity of Rotating Nuclear Medium

Ashutosh Dwibedi[1], Dani Rose J Marattukalam[1], Nandita
Padhan[2], Arghya Chatterjee[2] and Sabyasachi Ghosh[1]

[1]*Department of Physics, Indian Institute of Technology Bhilai,*
Kutelabhata, Durg, 491002, Chhattisgarh, India and

[2]*Department of Physics, National Institute of Technology Durgapur, Durgapur, 713209, West Bengal, India*

Following the recent observation of non-zero spin polarization and spin alignment of a few hadrons, the rotational aspect of quark-gluon plasma formed in heavy ion collisions has attracted considerable interest. The present work explores the effect of the Coriolis force, arising due to this rotation, on the shear viscosity of the medium. Using the relaxation time approximation within the kinetic theory framework, we analyze the parallel ($\eta_{||}/s$), perpendicular ($\eta_{\perp}/s$) and Hall ($\eta_{\times}/s$) components of shear viscosity to entropy density ratio under rotation. The estimation of anisotropic shear viscosity components is carried out using hadron resonance gas degrees of freedom below the critical (transition) temperature and massless partonic degrees of freedom above this temperature. Our results show that rotation suppresses the shear viscosity of the medium, with the degree of suppression depending on the ratio between the relaxation time and the rotational period. In the context of realistic heavy-ion collision experiments, the temperature and angular velocity both decrease with time, and one can establish a connection between them through the standard approximate cooling law. For a temperature-dependent angular velocity $\Omega(T)$, we obtain a traditional valley-like pattern for all components $\eta_{||}/s$, $\eta_{\perp}/s$ and $\eta_{\times}/s$ with reduced magnitudes compared to the valley-like isotropic η/s one encounters in the absence of rotation.

I. INTRODUCTION

The primary goal of the heavy ion collision (HIC) experiments performed in the Large Hadron Collider (LHC) and Relativistic Heavy Ion Collider (RHIC) is to study the properties of highly dense and hot quantum chromodynamics (QCD) matter [1, 2]. A plethora of theoretical and experimental studies have supported the formation of quark-gluon plasma (QGP) in the initial stage of the HIC, followed by a hadron gas phase. Many experimental observables, such as jet quenching [3], collective flow [4], nuclear suppression factor (R_{AA}) of heavy mesons [5] etc., show signs of the initial formation of QGP in HICs. It is worth mentioning that while the above-mentioned experimental observables have been well studied for the nuclear matter produced in HIC devoid of external electromagnetic fields and/or vorticity, their studies by including the latter effects have been less explored. The initial colliding nuclei of an off-central HIC can have a large orbital angular momentum (OAM), a fraction of which gets transferred to the quark-gluon medium [6–8]. Moreover, colliding nuclei being electrically charged and moving with ultra-relativistic velocity can create a huge transient magnetic field in the reaction zone. The dynamics of the QCD matter in the presence of magnetic fields and angular momentum opens up intense theoretical research in the field of HIC. To incorporate the effect of initial OAM in medium dynamics, two different treatments exist — in one approach, the OAM is taken to be stored in the medium locally in terms of fluid vorticity [9], whereas in the other approach, a globally rotating medium is considered by defining a transformation which links the inertial frame coordinates with corotating frame coordinates [10]. In the global rotation approach, the magnitude of angular velocity is essentially taken as the spatial average of the local vortices in the fluid [11]. There exists a list of seminal papers in which quantum field theory has been explored from a globally rotating frame [12–17]. Various other studies have considered different effective field-theoretical approaches on globally rotating QCD matter to investigate associated diverse rotational effects [18–31].

On the other hand, on the experimental side, there is enormous interest in looking for evidence of vorticity in the medium created in HICs. This vorticity manifests itself through the spin-orbit coupling, which can generate polarization or spin alignment along the direction of the vorticity in the local fluid cell. Averaged over the entire system, this polarization points along the direction of the angular momentum of the collision [7, 8]. A few years ago, the STAR collaboration made a precise measurement of the average polarization of Λ and $\bar{\Lambda}$ hyperons in mid-central collisions (20–50 % centrality) [6]. Since the polarization of Λ and $\bar{\Lambda}$ is solely carried by the strange quark, these measurements provided a direct probe of the rotational properties of the medium. The results revealed a positive, nonzero value for the polarization vector, offering compelling evidence for the existence of strong vorticity. Using the hydrodynamics relation, the measured $\sqrt{S_{NN}}$-averaged polarization values across $\sqrt{S_{NN}} = 7.7$ to 200 GeV correspond to average rotational vorticity of approximately $(9 \pm 1) \times 10^{21}$ per sec [6, 32]. Furthermore, as a function of collision energy, the polarization value decreases. This trend is also consistent with the hyperon global polarization measurement done by the ALICE collaboration for Pb-Pb collisions at $\sqrt{S_{NN}} = 2.76$ and 5.02 TeV [33]. Additionally, the spin alignment of vector mesons like ϕ and K^{*0} in HICs is linked to system vorticity, which may arise due to the large initial angular momentum of the system. Deviations in the spin density matrix element ρ_{00} from 1/3 indicate

finite global spin alignment, and recent experimental results from ALICE and STAR suggest that spin alignment can serve as a probe of vorticity of the medium [34, 35].

Apart from the spin polarization, which emerged as a necessary observable in recent times, the momentum and its affiliated transport coefficients, along with the equation of state (EoS) of the matter produced in HIC, play a vital role in the hydrodynamic evolution of the system. The transport coefficients of both partonic and hadronic matter in the absence of magnetic fields have been explored in Refs. [36–55]. In the presence of magnetic fields, the rotational symmetry of the medium breaks with the magnetic field vector $\vec{B}$, singling out a particular direction in space; as a result, the transport coefficients become anisotropic [56–66]. Same is true in case of a rotating medium, where the direction of angular velocity $\vec{\Omega}$ breaks the isotropy of the space. Recently, the anisotropic electrical conductivities [67] and shear viscosities [68] of a rotating gas in a non-relativistic framework and electrical conductivity of a rotating system of hadrons [69] in a relativistic framework have been analyzed. Moreover, the heavy quarks produced during the hard collision process may undergo an anisotropic spatial diffusion while traveling through the rotating medium, as pointed out in Ref. [70]. In this paper, by extending the previous work of Ref. [68], we have calculated the shear viscosity of the rotating nuclear matter in both the QGP and hadron gas phases. To fulfill this purpose, we use the Boltzmann transport equation (BTE) in the rotating frame with the collision kernel replaced by the relaxation time approximation (RTA). The rotating background has been incorporated through the rotating frame metric obtained by connecting the inertial coordinates with the corotating coordinates. In this way, the apparent forces appear in BTE in the form of connection coefficients, which in turn are expressed as the derivatives of the rotating frame metric. To keep the analysis simple, we consider the terms that are linear in the angular velocity in the BTE, which amounts to ignoring the centrifugal effects while keeping the effect of the Coriolis force. For the sake of simplicity, the QGP is modeled with a massless gas of quarks and gluons with constant relaxation time, whereas the hadron gas phase is modeled with the popular hadron resonance gas model (HRG) with a hard sphere scattering type interaction. The HRG model is highly successful in reproducing the thermodynamics of QCD matter below the critical point; therefore, it is also expected to give a realistic estimation of the transport coefficients at lower temperatures.

The article is arranged as follows: in Sec. II, we discuss the necessary formalism and obtain the expressions for different components of shear viscosity of QCD medium in a rotating frame. We then briefly address the HRG model and write down the final expressions for viscosities in the hadron gas phase in Sec. II A and the QGP phase in Sec. II B. In Sec. III, we discuss our results, particularly the temperature variation of anisotropic shear viscosity components of a rotating QCD matter both in the partonic and hadronic regimes. The analysis is carried out in two scenarios — one where we consider a medium globally rotating at a constant angular velocity and the other where a more realistic temperature-dependent angular velocity is considered. Finally, we summarize the article in Sec. IV.

II. FORMALISM

We start this section with a succinct recapitulation of the rotating kinetic theory model developed for the nuclear matter produced in off-central HIC within the non-relativistic setting in Refs. [67, 68] which was further generalized to the relativistic setting in Ref. [69]. By taking advantage of the fact that produced nuclear matter in off-central HIC can have a large initial OAM, we assume that the velocity of the medium particles has two effective parts: (1) a globally rotating part and (2) a random part on top of the global rotating part. This effective breaking of kinematic degrees of freedom for the matter helps one to write down the BTE in the globally rotating frame and solve for the distribution function f as a function of co-rotating space-time coordinates and momentum in the rotating frame.

The structure of BTE in general coordinates or in the presence of gravity depends on the metric tensor $g_{\mu\nu}$ and the connection coefficients $\Gamma^{\alpha}_{\beta\gamma}$. The co-rotating frame metric $g_{\mu\nu}$ can be readily obtained from the rotating coordinate transformation about $z-$axis as [23–25, 71],

$$g_{\mu\nu} = \begin{pmatrix} 1 - \Omega^2 x^2 - \Omega^2 y^2 & \Omega y & -\Omega x & 0 \\ \Omega y & -1 & 0 & 0 \\ -\Omega x & 0 & -1 & 0 \\ 0 & 0 & 0 & -1 \end{pmatrix}. \tag{1}$$

The space-dependent metric $g_{\mu\nu}$ essentially captures non-trivial space-time geometry in the rotating frame. Its derivative can be used to get the connection coefficients in the rotating frame as [72–74]:

$$\Gamma^{\alpha}_{\mu\lambda} = \frac{1}{2} g^{\alpha\nu} \left(\frac{\partial g_{\nu\mu}}{\partial x^{\lambda}} + \frac{\partial g_{\lambda\nu}}{\partial x^{\mu}} - \frac{\partial g_{\mu\lambda}}{\partial x^{\nu}} \right). \tag{2}$$

The only non-zero connection coefficients in our case are: $\Gamma^{1}_{00} = -\Omega^2 x, \Gamma^{2}_{00} = -\Omega^2 y, \Gamma^{1}_{20} = \Gamma^{1}_{02} = -\Omega, \Gamma^{2}_{10} = \Gamma^{2}_{01} = \Omega$. Due to the nature of the metric $g_{\mu\nu}$, which significantly differs from $\eta_{\mu\nu}$, the covariant and contravariant components of
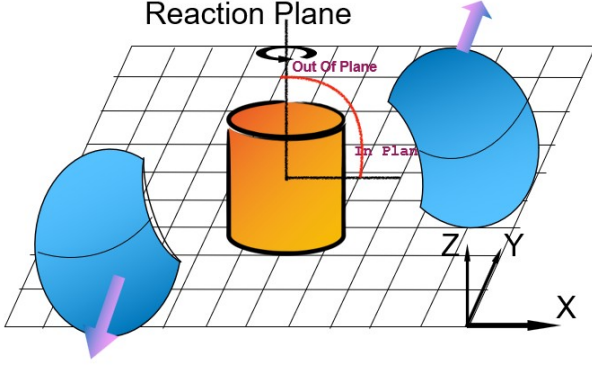
FIG. 1: Schematic representation of an off-central heavy-ion collision with OAM along the z-axis.
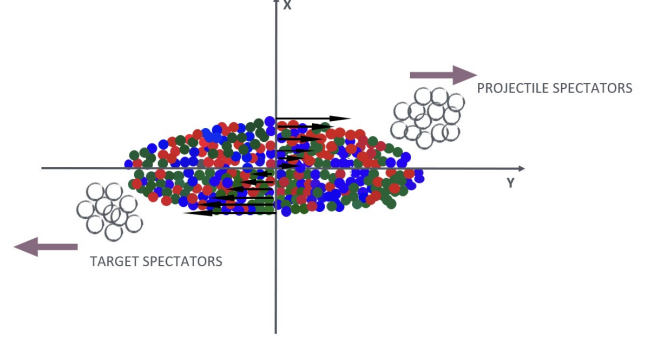
FIG. 2: Illustration of rotational patterns of partons in the reaction plane during off-central heavy-ion collisions.

the same vector will also differ significantly. The four momenta for the hadrons are expressed as: $p^\alpha = (\gamma_v m, \gamma_v m \vec{v}) = (\gamma_v m, \vec{p})$, where [74, 75],

$$\gamma_v \equiv \frac{dt}{d\tau} = \frac{1}{\sqrt{g_{00}(1 + \frac{g_{0i}v^i}{g_{00}})^2 - v^2}} \ , \tag{3}$$

with the following definitions used $v^i \equiv \frac{dx^i}{dt}$ and $v^2 \equiv (\frac{g_{0i}g_{0j}}{g_{00}} - g_{ij})v^i v^j$. Similarly, one can easily show,

$$p_0 \equiv g_{0\mu}p^\mu = E = \sqrt{m^2 g_{00} + (g_{0i}g_{0j} - g_{00}g_{ij})p^i p^j} \ . \tag{4}$$

The covariant BTE for the rotating hadronic medium reads as [76–78]:

$$p_r^\mu \frac{\partial f_r}{\partial x^\mu} - \Gamma_{\mu\lambda}^\alpha p_r^\mu p_r^\lambda \frac{\partial f_r}{\partial p_r^\alpha} + m_r F_r^\alpha \frac{\partial f_r}{\partial p_r^\alpha} = C[f_r] \ , \tag{5}$$

where F_r^α is the four force and $C[f_r]$ is the collision kernel which arises due to the random collision between hadrons. Here, we are interested in calculating the transport coefficients for the rotating hadronic matter in the absence of any external four forces. Therefore, we will have $F_r^\alpha = 0$ in Eq. (5). The usual assumption of solving the Boltzmann kinetic equation can then be employed to split the total distribution f_r into local equilibrium distribution f_r^0 and a perturbation δf_r, i.e., $f_r = f_r^0 + \delta f_r$. The local equilibrium distributions are given by, $f_r^0 = 1/[e^{(p_r^\alpha u^\beta g_{\alpha\beta} - \mu_r)/T} - \xi] = 1/[e^{(p_r^\alpha u_\alpha - \mu_r)/T} - \xi]$, where $\xi = -1$ for baryons and $\xi = +1$ for mesons. The four-vector u^μ, and the scalars μ_r and T occurring in the equilibrium distributions f_r^0 are identified with the fluid four-velocity, the chemical potential of the rth hadronic species and temperature. The perturbative correction δf_r to the local equilibrium distribution is assumed to be small, and it contains the thermodynamic forces that drive dissipative flows. As an application of the kinetic theory in the rotating frame, we will now proceed to derive the shear viscosity coefficients of the rotating hadronic matter.

For a rotating system of hadrons, the microscopic and macroscopic expression for viscous flow or viscous stress tensor τ^{ij} (this should not be confused with the average collision time τ_c between hadrons) can be written as,

$$\tau^{ij} = \sum_r \tau_r^{ij} = \sum_r g_r \int \frac{d^3\vec{p}_r}{(2\pi)^3} \frac{p_r^i p_r^j}{E_r} \delta f_r \ , \tag{6}$$

$$\tau^{ij} = -\sum_r \eta^{(r)ijkl} U^{kl} \equiv -\eta^{ijkl} U^{kl} \ , \tag{7}$$

where $U^{kl} = \frac{1}{2}(\frac{\partial u_k}{\partial x_l} + \frac{\partial u_l}{\partial x_k})$ is the fluid velocity gradient and η^{ijkl} is the viscosity tensor. The macroscopic expression of viscous stress tensor τ^{ij} provided in Eq. (7) is reminiscent of Newton's law of viscosity. This macroscopic expression can be compared with the microscopic kinetic theory expression provided in Eq. (6) for the determination of viscosity.

For the kinetic evaluation of the viscous tensor, we resort to the BTE in RTA. For a system of rotating hadrons, we can write the BTE in RTA as [76–79]:

$$p_r^\mu \frac{\partial f_r}{\partial x^\mu} - \Gamma_{\mu\lambda}^\alpha p_r^\mu p_r^\lambda \frac{\partial f_r}{\partial p_r^\alpha} = -(u^\alpha p_{r\alpha})\frac{f_r - f_r^0}{\tau_c} \ , \tag{8}$$

where τ_c is the average collision time between hadrons. In Eq. (8), the information of the rotating space-time background has been encoded in the connection coefficients $\Gamma_{\mu\lambda}^\alpha$. The second term of the LHS of Eq. (8) contains all the possible pseudo forces that can affect the transport properties of the system. Substituting the local equilibrium distribution f_r^0, in Eq. (8), we get the following linearized BTE,

$$-f^0(1 + \xi f^0)\left[\frac{p^\mu p^\alpha}{T}D_\mu u_\alpha + p^\mu(u_\alpha p^\alpha)\partial_\mu \frac{1}{T} - p^\mu \partial_\mu \frac{\mu}{T}\right] - \Gamma_{\mu\lambda}^\sigma p^\mu p^\lambda \frac{\partial \delta f}{\partial p^\sigma} = -(u^\alpha p_\alpha)\frac{f - f^0}{\tau_c} \ , \tag{9}$$

where we suppressed the index r, which will be retained during the calculation of shear viscosity. The covariant derivative D_μ of fluid velocity u_α is defined as $D_\mu u_\alpha \equiv \partial_\mu u_\alpha - \Gamma_{\mu\alpha}^\sigma u_\sigma$. In principle, Eq. (9) can be solved to obtain all the possible transport coefficients of the rotating hadron matter. Nevertheless, as pointed out in Ref. [69], the calculation involved becomes cumbersome because of the space-time dependence of the rotating metric $g^{\mu\nu}$. Therefore, in the present paper, we solve Eq. (9) with the same approximation which has been used in Ref. [69]. The approximation involves ignoring the second or higher powers of Ωx, Ωy, and $\frac{\Omega}{T}$, which is justified when one restricts oneself in a region that is closer to the axis of cylinder (or, away from the boundary of the causal cylinder, which is defined as the locus points satisfying $\Omega\sqrt{x^2 + y^2} = 1$) and angular velocity Ω is less than thermal energy scale ($\sim T$). In the static limit $u^\mu = (\frac{1}{\sqrt{g_{00}}}, 0)$ we have $\Gamma_{\mu\alpha}^\sigma u_\sigma = 0$ and $\frac{p^\mu p^\alpha}{T}\partial_\mu u_\alpha = -\frac{p^0 p^i}{T}\frac{\partial u^i}{\partial t} - \frac{p^i p^j}{T}\partial_j u^i$ giving,

$$-f^0(1 + \xi f^0)\quad\left[-\frac{p^0 p^i}{T}\frac{\partial u^i}{\partial t} - \frac{p^i p^j}{T}\partial_j u^i + p_0 p^0 \frac{\partial}{\partial t}\frac{1}{T} + p_0 p^i \partial_i \frac{1}{T} - p^0 \frac{\partial}{\partial t}\frac{\mu}{T} - p^i \partial_i \frac{\mu}{T}\right]$$
$$+ 2\Omega p^0\left(p^2 \frac{\partial \delta f}{\partial p^1} - p^1 \frac{\partial \delta f}{\partial p^2}\right) = -p_0 \frac{\delta f}{\tau_c}. \tag{10}$$

The time derivatives of μ/T, $1/T$, and u^i occurring in Eq. (10) can be eliminated with the help of conservation equations [76], and they finally contribute to the scalar (bulk viscous flow) and vector sector (thermal current) of the transport. Since the present paper is planned for the calculation of the shear viscosity, we can ignore the scalar and vectorial part of the thermodynamic fluxes occurring in the LHS of Eq. (10) to write,

$$f^0(1 + \xi f^0)\frac{p^i p^j}{ET}\partial_i u^j + 2(\vec{p} \times \vec{\Omega}) \cdot \frac{\partial \delta f}{\partial \vec{p}} = -\frac{\delta f}{\tau_c} \ , \tag{11}$$

where we assumed a rotation about the $z-$ axis, i.e., $\vec{\Omega} = \Omega\hat{k}$. Eq. (11) bears a formal resemblance to the one encountered in the computation of shear viscosity in the presence of a magnetic field. Therefore, it can be solved using a similar technique as employed in Ref. [80]. By using the definitions: $\tau_\Omega \equiv \frac{1}{2\Omega}$, $\vec{\Omega} \equiv \Omega\hat{\omega} \implies \Omega^i = \Omega\omega^i$, and $U^{ij} \equiv \frac{1}{2}(\frac{\partial u^i}{\partial x^j} + \frac{\partial u^j}{\partial x^i})$ we can rewrite Eq. (11) as:

$$f^0(1 + \xi f^0)\frac{p^i p^j}{ET}U^{ij} + \frac{1}{\tau_\Omega}\epsilon^{ijk}p^j\omega^k \frac{\partial \delta f}{\partial p^i} = -\frac{\delta f}{\tau_c} \ . \tag{12}$$

For the evaluation of viscous stress tensor and viscosity in Eq. (6) one has to solve Eq. (12) for δf. Here, we outline the steps to solve Eq. (12), delegating the detailed calculations to Appendix A. A quick glance at Eq. (12) suggests that the solution of δf should be proportional to two powers of momentum i.e., $\delta f \propto p^k p^l$ which leads to the most general guess $\delta f = \sum_{n=0}^{6} C_n C_n^{kl} p^k p^l$, where C_n are functions of energy along with other possible thermodynamic variables. The C_n^{kl} are the seven independent velocity gradients that one can construct with the help of the tensors: U^{ij}, δ^{ij}, and ϵ^{ijk}. Out of these seven independent tensors, the first five are traceless, and the other two have non-zero traces. The seven C_n^{kl} can be considered as the thermodynamic forces that drive dissipative flows in the rotating medium. The first five $C_n^{kl}(n = 0 \text{ to } 4)$ drive shear flows, and the respective proportionality factors are called shear viscosities, whereas the next two $C_n^{kl}(n = 5, 6)$ drive bulk flows and the respective proportionality factors are called bulk viscosities. The seven velocity gradients C_n^{ij} can be written as a combination of contraction of seven 4−rank tensors C_n^{ijkl} with U^{kl},

i.e., $C_n^{ij} \equiv C_n^{ijkl}U^{kl}$. Retaining the particle index r which we suppressed while transitioning from Eq. (8) to Eq. (9), the viscosity tensor for the rth hadronic species $\eta^{(r)ijkl}$ can be expressed in terms of the 4−rank tensors C_n^{ijkl} as,

$$
\begin{aligned}
\eta^{(r)ijkl} &= \eta_0^r C_0^{ijkl} + \eta_1^r C_1^{ijkl} + \eta_2^r C_2^{ijkl} + \eta_3^r C_3^{ijkl} + \eta_4^r C_4^{ijkl} \\
&\quad + \zeta_5^r C_5^{ijkl} + \zeta_6^r C_6^{ijkl},
\end{aligned} \tag{13}
$$

where η_n^r (for $n = 0$ to 4) and ζ_n^r (for $n = 5, 6$) are identified with shear and bulk viscosity coefficients, respectively. Using the macroscopic version of Newton's law provided in Eq. (7), we have,

$$
\tau^{ij} = -\sum_r \eta^{(r)ijkl} U^{kl} = -\sum_{n=0}^{4} \eta_n C_n^{ij} - \sum_{n=5}^{6} \zeta_n C_n^{ij}, \tag{14}
$$

where we defined the total shear and bulk viscosity coefficients of the rotating medium as the sum of the contributions from individual particles, i.e., $\eta_n = \sum_r \eta_n^r$ and $\zeta_n = \sum_r \zeta_n^r$. Since the present article is structured for the calculation of shear viscosity coefficients of the rotating QCD matter, we will keep only the terms that correspond to shear stress tensor or shear flow in Eq. (6) and Eq. (14) and rewrite them as follows:

$$
\pi^{ij} = \sum_r g_r \int \frac{d^3\vec{p}_r}{(2\pi)^3} \frac{p_r^i p_r^j}{E_r} \delta f_r , \tag{15}
$$

$$
\pi^{ij} = -\sum_{n=0}^{4} \eta_n C_n^{ij} . \tag{16}
$$

For the kinetic evaluation of the shear flow π^{ij} we will substitute $\delta f_r = \sum_{n=0}^{4} C_n^r C_n^{kl} p_r^k p_r^l$ in Eq. (15) to obtain,

$$
\begin{aligned}
\pi_{ij} &= \sum_r g_r \int \frac{d^3\vec{p}}{(2\pi)^3 E} \sum_{n=0}^{4} C_n C_n^{kl} \, p^i p^j p^k p^l \\
\implies \quad \pi_{ij} &= \sum_r g_r \int \frac{d^3 p}{(2\pi)^3 E} \sum_{n=0}^{4} C_n C_n^{kl} (\delta^{ij}\delta^{kl} + \delta^{ik}\delta^{jl} + \delta^{il}\delta^{jk}) \frac{p^4}{15} \\
\implies \quad \pi_{ij} &= \sum_{n=0}^{4} C_{ij}^n \sum_r \frac{2g_r}{15} \int \frac{d^3 p}{(2\pi)^3 E} C_n \, p^4,
\end{aligned} \tag{17}
$$

where for the notational simplicity we suppressed the particle index r in the unknown coefficients C_n and momentum components p^i. We also used the identities, $\int p^i p^j p^k p^l d^3\vec{p} = \int \frac{p^4}{15}(\delta^{ij}\delta^{kl} + \delta^{ik}\delta^{jl} + \delta^{il}\delta^{jk})d^3 p, (d^3 p \equiv 4\pi p^2 dp)$ and $C_{kl}^n(\delta^{ij}\delta^{kl} + \delta^{ik}\delta^{jl} + \delta^{il}\delta^{jk}) = 2C_{ij}^n$. The unknown coefficients C_n appearing in Eq. (17) are explicitly calculated in Appendix A. Using the expression of C_n obtained in Eq. (A7) and comparing it with Eq. (16) we obtain the following expressions for shear viscosity components,

$$
\eta_1 = \sum_r \frac{g_r}{15T} \frac{\tau_c}{1 + 4(\tau_c/\tau_\Omega)^2} \int \frac{d^3 p}{(2\pi)^3} \frac{p^4}{E^2} f^0(1 + \xi f^0)
$$

$$
\eta_2 = \sum_r \frac{g_r}{15T} \frac{\tau_c}{1 + (\tau_c/\tau_\Omega)^2} \int \frac{d^3 p}{(2\pi)^3} \frac{p^4}{E^2} f^0(1 + \xi f^0)
$$

$$
\eta_3 = \sum_r \frac{g_r}{15T} \frac{2\tau_c(\tau_c/\tau_\Omega)}{1 + 4(\tau_c/\tau_\Omega)^2} \int \frac{d^3 p}{(2\pi)^3} \frac{p^4}{E^2} f^0(1 + \xi f^0)
$$

$$
\eta_4 = \sum_r \frac{g_r}{15T} \frac{\tau_c(\tau_c/\tau_\Omega)}{1 + (\tau_c/\tau_\Omega)^2} \int \frac{d^3 p}{(2\pi)^3} \frac{p^4}{E^2} f^0(1 + \xi f^0) \tag{18}
$$

The shear viscosity component in the absence of rotation $\eta_0 \equiv \eta$ is given by [80],

$$
\eta_0 = \sum_r \frac{g_r}{15T} \tau_c \int \frac{d^3 p}{(2\pi)^3} \frac{p^4}{E^2} f^0(1 + \xi f^0) \tag{19}
$$

One can define the perpendicular $\eta_\perp$, parallel $\eta_\parallel$ and Hall $\eta_\times$ viscosity as [80], $\eta_1 \equiv \eta_\perp$, $\eta_2 \equiv \eta_\parallel$, and $\eta_4 \equiv \eta_\times$.

A. Shear viscosity for HRG

The hadronic phase of matter created in HICs can be effectively described by HRG model [81–86]. This model is widely accepted in the community for the characterization of the thermodynamics [87, 88], conserved charge fluctuations [89–93], as well as transport coefficients [36, 37, 42, 94–101] of the created hadron gas in HICs. The HRG model offers a grand canonical ensemble treatment of the hadron gas by including all the degrees of freedom associated with the system, i.e., hadrons and their resonances. It has been shown by the S-matrix calculation that in the presence of narrow resonances, the interacting gas of hadrons can be approximated by an ideal gas comprising of hadrons and their resonances [102, 103]. Here, we will model the hadron gas by an ideal gas of non-interacting point-like hadrons and resonances up to mass 2.6 GeV as listed in Ref. [104]. In the grand canonical ensemble approach of the ideal HRG model, one expresses grand potential ϕ_G as [105],

$$-P^{\mathrm{HRG}}\, V = \Phi_G = -T\sum_B \frac{V g_B}{2\pi^2}\int p^2 dp\, \ln\left[1+e^{-E_B/T}\right] + T\sum_M \frac{V g_M}{2\pi^2}\int p^2 dp\, \ln\left[1-e^{-E_M/T}\right], \tag{20}$$

where we consider zero chemical potential for all hadrons with two separate summations for baryons (B) and mesons (M). In Eq. (20), m_B, $E_B = \sqrt{p^2 + m_B^2}$, and $g_B = 2S_B + 1$ are equal to the mass, energy, and spin degeneracy of the baryons with spin S_B, respectively. Similarly, we have m_M, $E_M = \sqrt{p^2 + m_M^2}$, $g_M = 2S_M + 1$ equal to the mass, energy, and spin degeneracy of the mesons with spin S_M, respectively. The entropy density can be obtained from Eq. (20) as,

$$s^{\mathrm{HRG}} = -\frac{1}{V}\frac{\partial \Phi_G}{\partial T} = \frac{\mathcal{E}^{HRG} + P^{\mathrm{HRG}}}{T}, \tag{21}$$

where energy density $\mathcal{E}^{\mathrm{HRG}}$ and pressure P^{HRG} of the HRG are given by,

$$\mathcal{E}^{\mathrm{HRG}} = \sum_B \frac{g_B}{2\pi^2}\int \frac{p^2 dp}{e^{E_B/T}+1}E_B + \sum_M \frac{g_M}{2\pi^2}\int \frac{p^2 dp}{e^{E_M/T}-1}E_M, \tag{22}$$

$$P^{\mathrm{HRG}} = \sum_B \frac{g_B}{2\pi^2}\int \frac{p^2 dp}{e^{E_B/T}+1}\left(\frac{p^2}{3E_B}\right) + \sum_M \frac{g_M}{2\pi^2}\int \frac{p^2 dp}{e^{E_M/T}-1}\left(\frac{p^2}{3E_M}\right). \tag{23}$$

Similarly, we can express the shear viscosity components given in Eqs. (19) and (18) by two separate the summation for baryons (B) and mesons (M) as follows,

$$\eta_0^{\mathrm{HRG}} \equiv \eta^{\mathrm{HRG}} = \sum_B \frac{g_B}{15T}\int \frac{d^3 p}{(2\pi)^3}\tau_c^B \times \frac{p^4}{E_B^2}f_B^0(1-f_B^0) + \sum_M \frac{g_M}{15T}\int \frac{d^3 p}{(2\pi)^3}\tau_c^M \times \frac{p^4}{E_M^2}f_M^0(1+f_M^0) \tag{24}$$

$$\eta_1^{\mathrm{HRG}} = \eta_\perp^{\mathrm{HRG}} = \sum_B \frac{g_B}{15T}\int \frac{d^3 p}{(2\pi)^3}\frac{\tau_c^B}{1+4(\tau_c^B/\tau_\Omega)^2}\times\frac{p^4}{E_B^2}f_B^0(1-f_B^0)$$

$$+\sum_M \frac{g_M}{15T}\int \frac{d^3 p}{(2\pi)^3}\frac{\tau_c^M}{1+4(\tau_c^M/\tau_\Omega)^2}\times\frac{p^4}{E_M^2}f_M^0(1+f_M^0) \tag{25}$$

$$\eta_2^{\mathrm{HRG}} = \eta_\|^{\mathrm{HRG}} = \sum_B \frac{g_B}{15T}\int \frac{d^3 p}{(2\pi)^3}\frac{\tau_c^B}{1+(\tau_c^B/\tau_\Omega)^2}\times\frac{p^4}{E_B^2}f_B^0(1-f_B^0)$$

$$+\sum_M \frac{g_M}{15T}\int \frac{d^3 p}{(2\pi)^3}\frac{\tau_c^M}{1+(\tau_c^M/\tau_\Omega)^2}\times\frac{p^4}{E_M^2}f_M^0(1+f_M^0) \tag{26}$$

$$\eta_4^{\mathrm{HRG}} = \eta_\times^{\mathrm{HRG}} = \sum_B \frac{g_B}{15T}\int \frac{d^3 p}{(2\pi)^3}\frac{\tau_c^B(\tau_c^B/\tau_\Omega)}{1+(\tau_c^B/\tau_\Omega)^2}\times\frac{p^4}{E^2}f_B^0(1-f_B^0)$$

$$+\sum_M \frac{g_M}{15T}\int \frac{d^3 p}{(2\pi)^3}\frac{\tau_c^M(\tau_c^M/\tau_\Omega)}{1+(\tau_c^M/\tau_\Omega)^2}\times\frac{p^4}{E_M^2}f_M^0(1+f_M^0), \tag{27}$$

where $f_B^0 = 1/(e^{E_B/T}+1)$, $f_M^0 = 1/(e^{E_M/T}-1)$, and $\tau_c^{B,M}$ are the relaxation times of hadrons (baryons and mesons). The relaxation time for any hadron facing the total number density n_{HRG} can be determined by resorting to the hard-sphere scattering model,

$$\tau_c^{B,M} = \frac{1}{n_{\mathrm{HRG}}\, v_{\mathrm{av}}^{B,M}\, \pi a^2}, \tag{28}$$

where $v_{\text{av}}^{B,M}$ for any hadron is given by,

$$v_{\text{av}}^{B,M} = \int \frac{d^3p}{(2\pi)^3} \frac{p}{E_{B,M}} f_0^{B,M} \bigg/ \int \frac{d^3p}{(2\pi)^3} f_0^{B,M} , \tag{29}$$

and the total number density for the HRG is expressed as,

$$n_{\text{HRG}} = \sum_B g_B \int \frac{d^3p}{(2\pi)^3} f_B^0 + \sum_M g_M \int \frac{d^3p}{(2\pi)^3} f_M^0 . \tag{30}$$

B. Shear viscosity for massless QGP

We can get the shear viscosity components for a massless rotating QGP by replacing p by E and summing over the quark (q) and gluon (g) degrees of freedom with appropriate degeneracies in Eqs. (18) and (19) as,

$$
\begin{aligned}
\eta_0^{\text{QGP}} \equiv \eta^{\text{QGP}} &= \frac{g_q \tau_c}{15T} \int \frac{d^3p}{(2\pi)^2} \frac{p^4}{E^2} f_q^0 (1 - f_q^0) + \frac{g_g \tau_c}{15T} \int \frac{d^3p}{(2\pi)^2} \frac{p^4}{E^2} f_g^0 (1 + f_g^0) \\
&= \frac{g_q \tau_c}{30\pi^2 T} \int dE\, E^4 f_q^0 (1 - f_q^0) + \frac{g_g \tau_c}{30\pi^2 T} \int dE\, E^4 f_g^0 (1 + f_g^0) \\
&= \frac{\tau_c T^4}{30\pi^2} 24T \frac{\partial}{\partial \mu} (g_q f_5^{\text{FD}}(A) + g_g f_5^{\text{BE}}(A)), \left(\text{where, } f_j^{\text{FD/BE}}(A) = \frac{1}{\Gamma(j)} \int_0^\infty \frac{x^{j-1} dx}{A^{-1} e^x \pm 1}, (A \equiv e^{\mu/T}) \right) \\
&= \frac{4\tau_c T^4}{5\pi^2} \left(g_q f_4^{\text{FD}}(1) + g_g f_4^{\text{BE}}(1) \right) \qquad \text{(by assuming } \mu = 0, A = 1) \\
&= \frac{4\tau_c T^4}{5\pi^2} \left(g_q \left(1 - \frac{1}{2^{4-1}} \right) + g_g \right) \zeta(4) \\
&= \frac{4\tau_c T^4}{5\pi^2} \left[\frac{7}{8} g_q + g_g \right] \zeta(4) = \frac{19\pi^2}{45} \tau_c T^4
\end{aligned} \tag{31}
$$

where we used $g_q = 3(\text{flavor}) \times 3(\text{color}) \times 2(\text{spin}) \times 2(\text{particle} - \text{antiparticle}) = 36$, $g_g = 2(\text{polarization}) \times 8(\text{color}) = 16$ and the $\zeta(4) = \frac{\pi^4}{90}$. Similarly, one can express the perpendicular, parallel, and Hall viscosities as,

$$\eta_{\perp,||,\times}^{\text{QGP}} = \eta_{1,2,4}^{\text{QGP}} = \frac{19\pi^2}{45} \tau_c^{\perp,||,\times} T^4 , \tag{32}$$

where the effective relaxation times for perpendicular, parallel and hall viscosities are defined as $\tau_c^\perp = \frac{\tau_c}{1 + 4(\tau_c/\tau_\Omega)^2}$, $\tau_c^{||} = \frac{\tau_c}{1 + (\tau_c/\tau_\Omega)^2}$, and $\tau_c^\times = \frac{\tau_c(\tau_c/\tau_\Omega)}{1 + (\tau_c/\tau_\Omega)^2}$. Entropy density s^{QGP} for the rotating QGP can be written as:

$$s^{\text{QGP}} = \frac{\mathcal{E}^{\text{QGP}} + P^{\text{QGP}}}{T} , \tag{33}$$

where $\mathcal{E}^{\text{QGP}}$ and P^{QGP} are the energy density and pressure of the QGP respectively. The pressure of the QGP can be evaluated as,

$$
\begin{aligned}
P^{\text{QGP}} &= g_q \int \frac{d^3p}{(2\pi)^3} \frac{p^2}{3E} f_q^0 + g_g \int \frac{d^3p}{(2\pi)^3} \frac{p^2}{3E} f_g^0 \\
&= \frac{1}{6\pi^2} \left[g_q \int dE E^3 f_q^0 + g_g \int dE E^3 f_g^0 \right] \\
&= \frac{T^4}{\pi^2} \left[g_q \left(1 - \frac{1}{2^3} \right) + g_g \right] \zeta(4) = \frac{19\pi^2}{36} T^4 .
\end{aligned} \tag{34}
$$

Using the fact that $\mathcal{E}^{\text{QGP}} = 3P^{\text{QGP}}$ along with Eqs. (33) and (34) we have,

$$s^{\text{QGP}} = \frac{19\pi^2}{9} T^3. \tag{35}$$

We assume the relaxation time in the QGP phase to be a temperature-independent constant, which is in good agreement with the other model calculations, as we will see in the next section.
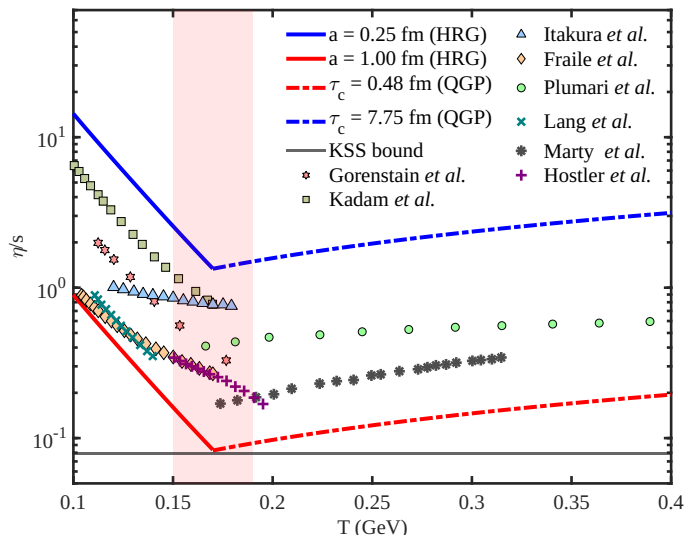
FIG. 3: (Color online) The variation of shear viscosity to entropy density ratio (η/s) with temperature comparing results from different previous model calculations (Gorenstein *et al.* [37], Kadam *et al.* [36], Itakura *et al.* [38], Fraile *et al.* [39], Plumari *et al.* [40], Lang *et al.* [41], Marty *et al.* [53], Hostler *et al.* [42]) along with the KSS bound obtained from AdS/CFT correspondence. RTA curves for massless QGP and HRG from our calculation to fit these results with parametrized relaxation time τ_c (with a hard sphere scattering length a) in the HRG phase and a constant τ_c in the QGP phase is given in the figure. The critical temperature is taken to be 0.17 GeV.

III.   RESULTS AND DISCUSSION

In this section, our primary objective is to explore the influence of rotation, specifically the Coriolis force, on shear viscosity. We compute the parallel, perpendicular, and Hall components of shear viscosity for the hadron gas phase using Eqs. (24)-(27) given in Sec. II A and for the QGP phase using Eqs. (31)-(32) given in Sec. II B. For our investigation of shear viscosity within rotating hadronic matter, we employ the HRG model, incorporating a comprehensive spectrum of hadrons and their resonances with masses up to 2.6 GeV [104] while we consider the rotating QGP phase to be a massless gas of quarks and gluons.

Fig. (3) illustrates the temperature dependence of shear viscosity-to-entropy density ratio (η/s) for both the hadronic and QGP phases using the relaxation time approximated kinetic theory framework. Several previous microscopic estimates [36–42, 53] of shear viscosity-to-entropy density ratio (η/s) can be found in the literature employing various effective and quasiparticle theories of QCD matter. Results obtained in Gorenstein *et al.* (VDW-HRG) [37], Kadam *et al.* (HRG-HS) [36], Itakura *et al.* (pion gas) [38], Fraile *et al.* (ChPT) [39], Plumari *et al.* (gluon plasma-RTA) [40], Lang *et al.* (pion gas) [41], Marty *et al.* (DQPM) [53], Hostler *et al.* (VDW-HRG) [42] are shown in the figure. The theoretical lower limit on the shear viscosity-to-entropy density ratio – the KSS bound ($\eta/s \geq 1/4\pi$) – obtained from AdS/CFT correspondence [106] is also indicated for reference.

By using the HRG model in the hadronic domain and the massless QGP case in the quark temperature domain, we have attempted to cover the data of these earlier works. To do this, we have tuned our τ_c to obtain the upper and lower limits. The relaxation time τ_c is fixed at a temperature-independent constant value in the QGP phase, whereas in the hadronic phase, the relaxation time, which depends on both temperature and scattering length, is determined using Eq. (28). The maximum and minimum values of τ_c in the QGP phase and scattering length a in the hadronic phase are tuned such that they are analytically continuous at T_c to make it visually appealing, but the reader should be careful about the scientific uncertainty in the shaded region near T_c.

For the purpose of this work, we assume the critical temperature to be $T_c = 170$ MeV. The HRG model is used to obtain results in the hadronic regime below T_c, while a gas of massless quarks and gluons is considered in the QGP regime above T_c. The shaded region around the quark-hadron phase transition temperature $T_c \approx 170$ MeV is used to remind the reader that the motivation of the present work is to provide a broad illustration of the shear viscosity across both phases. Although we have smoothly matched the estimations in the two phases at $T = 170$ MeV, our analysis mainly focuses on the order of magnitude and general trends of shear viscosity components outside this shaded region. This is because the region around the transition temperature can involve several uncertainties, such as (1) the precise location of the transition temperature—especially when using two different models for the two phases—and (2) how the transition temperature may be affected by rotation.
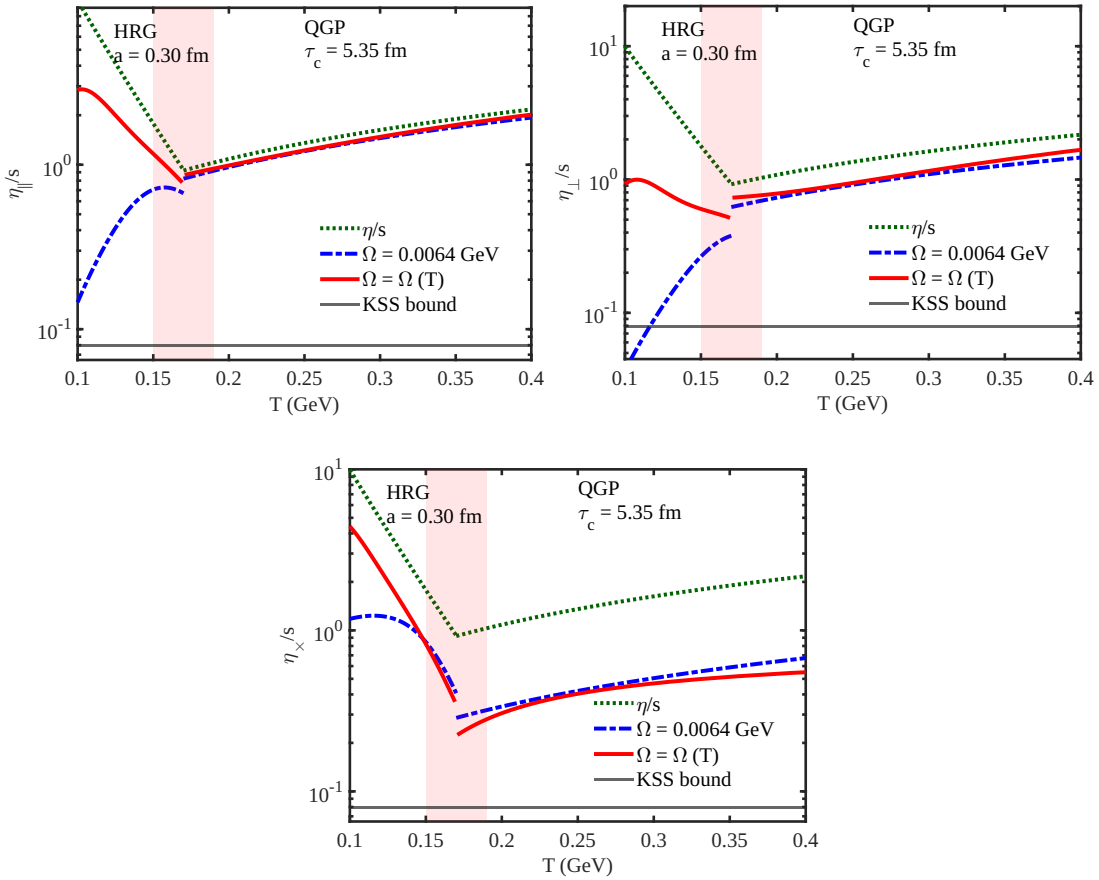
FIG. 4: (Color online) The variation of components of shear viscosity to entropy ratio $(\eta_{||}/s, \eta_{\perp}/s, \eta_{\times}/s)$ with temperature for a constant angular velocity $\Omega = 0.0064$ GeV (blue dash-dot curves) and a temperature-dependent angular velocity $\Omega = \Omega(T)$ (red solid curve) are compared with the estimates in the absence of rotation (green dotted curves). The critical temperature is taken to be 0.17 GeV.

To encompass a range of earlier η/s estimations obtained without considering rotation, from various effective transport models, we span the scattering length from 0.25 fm to 1 fm in the hadronic phase, while the relaxation time is varied from 0.48 to 7.75 fm in the QGP phase, as shown in Fig. (3). The red (blue) solid curves give the lower (upper) limit from our relaxation time approximated kinetic theory estimates in the HRG domain, and the red (blue) dot-dashed curves give the lower (upper) limit in the QGP phase. The behavior of η/s reveals a decreasing trend in the hadronic phase, while in the QGP phase, they increase monotonically. After calibrating the relaxation time and scattering length in Fig. (3), we will now move on to describe the effect of Coriolis force and anisotropic components of shear viscosity $(\eta_{||,\perp,\times})$ in Fig. (4).

Fig. (4) depicts the temperature dependence of the anisotropic components of the shear viscosity-to-entropy density ratio $(\eta_{||,\perp,\times}/s)$ under rotational effects in both the hadronic and QGP phases. To depict the variation of viscosity in the hadronic phase, we choose a scattering length of $a = 0.30$ fm, which falls in the band of scattering length obtained in Fig. (3). In the QGP phase, thermal relaxation time $\tau_c = 5.35$ fm is chosen. The impact of rotation is analyzed for two cases: a constant angular velocity ($\Omega = 0.0064$ GeV) and a temperature-dependent angular velocity $\Omega = \Omega(T)$. The temperature dependency of Ω can be roughly constructed as follows. In typical HIC experiments, some amount of OAM gets transferred to the medium, and the medium acquires some initial average angular velocity Ω. Since the medium expands with time, its momentum of inertia (I) increases, and therefore, the average angular velocity Ω should decrease to keep the angular momentum $L \sim I\Omega$ conserved. As the medium expands in time, it also cools; therefore, the Ω should decrease with T. The heuristic argument presented above will now be explored systematically. For the temperature-dependent angular velocity profile, let us use the parametrization of averaged vorticity as a function of time, centrality, and beam energy, given by Jiang et $al.$ [107] using multiphase transport (AMPT) model simulations,

$$\langle\omega_y\rangle(t, b, \sqrt{s_{NN}}) = A(b, \sqrt{s_{NN}}) + B(b, \sqrt{s_{NN}})(0.58t)^{0.35}e^{-0.58t}, \tag{36}$$

with the two coefficients A and B given by

$$A = \left[e^{-0.016b\sqrt{s_{NN}}} + 1\right] \times \tanh(0.28\,b) \times [0.001775\tanh(3 - 0.015\sqrt{s_{NN}}) + 0.0128]\,, \tag{37}$$

$$B = \left[e^{-0.016b\sqrt{s_{NN}}} + 1\right] \times [0.02388\,b + 0.01203] \times [1.751 - \tanh(0.01\sqrt{s_{NN}})]\,. \tag{38}$$

where $\sqrt{s_{NN}}$ is measured in GeV, b in fm, t in fm/c, and ω_y in fm^{-1}. In this context the angular velocity is given by $\Omega \equiv \frac{1}{2}\langle\omega_y\rangle$[1]. To approximately relate the temperature evolution of the fireball with its time evolution, we employ the Bjorken's scaling solution to describe the longitudinal expansion as

$$T(t) = T_0 \left(\frac{t}{t_0}\right)^{-1/3}\,. \tag{39}$$

In this analysis, we consider a fireball evolution corresponding to a collision at beam energy $\sqrt{S_{NN}} = 200$ GeV with an impact parameter $b = 5$ fm. The intial conditions are taken as an initial temperature $T_0 = 0.4$ GeV and initial time $t_0 = 0.14$ fm/c.

Now let us analyze the variation of anisotropic shear viscosity-to-entropy density ratio $(\eta_{\|,\perp,\times}/s)$ as a function of temperature as displayed in Fig. (4). For comparison, each plot also includes the isotropic shear viscosity component, $\eta \equiv \eta_0$, shown by the green dotted curve. The constant angular velocity $\Omega = 0.0064$ GeV$= 0.0325$ fm^{-1} (or, $\tau_\Omega = 15.39$ fm) is used in this analysis. This represents the maximum possible angular velocity provided by Eq. (36) for a collision at $\sqrt{S_{NN}} = 200$ GeV with $b = 5$ fm. As seen in the QGP phase ($T > 0.17$ GeV), the parallel component $\eta_\||/s$ with fixed angular velocity $\Omega = 0.0064$ GeV (blue dash-dot curve) lies slightly below the corresponding result with temperature-dependent angular velocity $\Omega(T)$ (red solid curve). Both anisotropic results are marginally lower than the isotropic η/s (green dotted curve). In the HRG phase, the ordering of the viscosity magnitudes are same as of the QGP phase, i.e., $\eta_\||(\Omega = 0.0064)/s$ (blue dash-dot curve) $< \eta_\||(\Omega(T))/s$ (red solid curve) $< \eta/s$ (green dotted curve) with significant difference in their magnitudes. These results can be mathematically understood by comparing the rotational time scale $\tau_\Omega(T)$ with the relaxation time scale $\tau_c(T)$, which are present in the expressions of $\eta_\||$. The effective relaxation times $\tau_c^{\||}(\Omega = 0.0064) < \tau_c^{\||}(\Omega(T))$ make the blue dash-dot curve lie below the red solid one. The upper right panel of Fig. (4) describes the same physics for the perpendicular component of viscosity. A comparison with $\eta_\||/s$ suggest that the magnitude $\eta_\perp/s$ is lesser than $\eta_\||/s$. This trend can also be understood from their respective expressions (25) and (26), which implies $\eta_\||(T)/s > \eta_\perp(T)/s$ as $\tau_c^{\||} > \tau_c^{\perp}$. The figure in the lower panel depicts the variation of Hall viscosity $\eta_\times/s$ with respect to temperature. One can observe a finite Hall component of viscosity both in the QGP and HRG phases as a result of rotation. In the temperature-dependent variation of $\eta_{\|,\perp,\times}/s$, we observed QGP-phase viscosity components for constant $\Omega = 0.0325$ fm^{-1} (corresponding to blue dash-dot curve) and for the temperature-dependent $\Omega(T)$ (red solid curve) nearly coincide, whereas a notable difference is seen in the hadronic phase. This behavior can be understood by falling back to the expressions (36) and (39). These equations indicate a smaller band of $\tau_\Omega \sim 15.39 - 20$ fm for the QGP temperature range $T = 0.4 - 0.17$ GeV but a larger band of $\tau_\Omega \sim 20 - 84$ fm for the HRG temperature domain $T = 0.7 - 0.1$ GeV. To summarize, for all three plots shown in Fig. (4), the key factor determining the shape and magnitude of the anisotropic viscosities is the ratio between the average thermal relaxation time τ_c and rotational time scale τ_Ω. To clarify the behavior observed in Fig. (4), we re-express the anisotropic viscosity components given in Eqs. (25), (26), and (27) for the HRG phase in a more transparent form. For this, we write the viscosity as a sum over contributions form baryons and mesons, and it is expressed as the product of two independent factors as follows,

$$\eta_{\perp,\||,\times}^{\text{HRG}}(T) = \sum_{B,M} \left(\tau_c^{\perp,\||,\times}\right)^{B,M} (\text{P.S})_\eta^{B,M}\,,$$

where the phase space part denoted as P.S is the same for different components of viscosity and only depends on temperature; on the other hand, the relaxation part has a different structure for different components of the viscosity. The effective relaxation times which modulates the thermal relaxation time $\tau_c(T)$ are given by, $(\tau_c^{\perp})^{B,M} = \frac{\tau_c^{B,M}(T)}{1+4(\tau_c^{B,M}(T)/\tau_\Omega(T))^2}$, $(\tau_c^{\||})^{B,M} = \frac{\tau_c^{B,M}(T)}{1+(\tau_c^{B,M}(T)/\tau_\Omega(T))^2}$, and $(\tau_c^{\times})^{B,M} = \frac{\tau_c^{B,M}(T)\,(\tau_c^{B,M}(T)/\tau_\Omega(T))}{1+(\tau_c^{B,M}(T)/\tau_\Omega(T))^2}$. The phase space part is $(\text{P.S})_\eta^{B,M} = \frac{g_{B,M}}{15T}\int\frac{d^3p}{(2\pi)^3}\tau_c^{B,M} \times \frac{p^4}{E_{B,M}^2}f_{B,M}^0(1\pm f_{B,M}^0)$, where $-$ is for baryons and $+$ mesons. Similarly, for components of the shear viscosities in the QGP phase, the relaxation part and phase space part are easily seen from Eq. (32).

---

[1] In Refs. [107], $y-$ axis is chosen perpendicular to the reaction plane whereas we have defined $z-$ axis to be perpendicular to the reaction plane (cf. Fig. 1).

It is worth mentioning that our results at finite rotation are similar to those obtained at finite magnetic field [54, 80], and we can explore their phenomenological connections. In the RTA-based kinetic theory framework, the Coriolis force in the presence of rotation and the Lorentz force in the presence of magnetic fields induces anisotropy in transport coefficients including shear viscosity. In the present work, based on the HRG model for hadronic temperature range and massless QGP case for quark temperature range, we notice a significant reduction in $\eta_{||}$ and $\eta_\perp$. The percentage reduction in the parallel and perpendicular components $\left(\frac{\eta - \eta_{||,\perp}}{\eta} \times 100\% \right)$ for the case temperature dependent $\Omega = \Omega(T)$ shown in Fig. (4) is as follows: the reduction in $\eta_{||}$ is about $6 - 10\%$ in the quark temperature range and $20 - 70\%$ in the hadron temperature range, while the reduction in $\eta_\perp$ is about $20 - 30\%$ in the quark temperature range and $45 - 90\%$ in the hadron temperature range. A similar reduction in $\eta_{||,\perp}/s$ is also noticed for the finite magnetic field picture. From the phenomenological point of view, as we move from head-on to peripheral collisions, we obtain a non-zero magnetic field and rotation. Our work suggests that the shear viscosity to entropy density ratio will have smaller values in peripheral collisions as compared to the corresponding estimates in head-on collisions. Lorentz force at finite magnetic field can lead to azimuthal anisotropy [108, 109], and similar effects are expected due to Coriolis force at finite rotation. To investigate the phenomenology of the magneto-rotational effects, including azimuthal anisotropy, a systematic hydrodynamic evolution at finite magnetic field and rotation with the inclusion of all viscosity components is required. Comparing experimental data from peripheral and head-on collisions may reveal signatures of finite magnetic field and rotation. To isolate the effect of rotation, the Hall component can serve as a useful probe since it vanishes for $\mu = 0$ at finite magnetic fields.

IV. SUMMARY

In the peripheral heavy ion collision experiments, some amount of initial angular momentum gets transferred to the formed quark-gluon plasma. By assuming a rotating plasma to account for this initial angular momentum, we set up a relativistic Boltzmann equation for the determination of its shear viscosities. The Coriolis force obtained from the non-trivial connection coefficients in the rotating frame enters the Boltzmann equation and makes the shear viscosities anisotropic. Using the Boltzmann equation in the rotating frame, we obtained five different components of shear viscosities. The different components of the shear viscosity obtained can be directly compared with the anisotropic shear viscosities one finds in the presence of magnetic fields where, in place of the angular velocity vector, the magnetic field vector breaks the isotropic nature of transport coefficients. To get a realistic estimate of the shear viscosities below the critical temperature, we employed the hadron resonance gas model, whereas, above the critical temperature, we took massless non-interacting partons as our degrees of freedom for the calculation of the shear viscosities. A compilation of previous microscopic estimates of shear viscosity to entropy density ratio gives a well-known valley-like pattern against the temperature axis with a minimum at the transition temperature. By tuning relaxation time in our model, we have obtained the upper and lower curves that can span these theoretical data. The relaxation time for the HRG phase was assumed to be given by hard sphere scattering interactions with tunable scattering length. In the QGP phase, we assumed a constant temperature-independent relaxation time. Once tuned to match previous estimates of the isotropic viscosity-to-entropy density ratio, the finite rotation extension gives a transformation from an isotropic to an anisotropic structure, characterized by three physical components: parallel, perpendicular, and Hall. The behavior of these anisotropic components is governed by two parts: an effective relaxation time that depends on both angular velocity and temperature and a phase space factor that is purely temperature-dependent. The average vorticity or angular velocity of the nuclear matter mostly decreases as the system cools with time. To see the actual variation of shear viscosity with temperature, we obtained the angular velocity as a function of temperature with the help of an approximate cooling law. In the same plot, we also showed the results with a constant angular velocity for comparison. We observe that the parallel and perpendicular components of the shear viscosity to entropy density ratio reduce due to rotation. The valley-like signature of the temperature dependence of shear viscosity is no longer valid if we consider a constant angular velocity throughout the evolution. However, with the realistic temperature-dependent angular velocity, the valley-like structure of temperature dependence of shear viscosity to entropy density ratio remains, though with a reduced magnitude. We would like to highlight that the present work is the first-of-its-kind attempt at characterizing the temperature dependence of shear viscosity components at finite rotation.

V. ACKNOWLEDGEMENT

Appendix A: Calculation of shear stress tensor

In this appendix we explicitly solve Eq. (12) to get the unknown coefficients C_n needed for the calculation of shear stress tensor provided in Eq. (17).

$$\frac{p^i p^j}{ET} U^{ij} f_0 (1 + \xi f_0) + \frac{1}{\tau_\Omega} \epsilon^{ijk} p^j \omega^k \frac{\partial \delta f}{\partial p^i} = -\frac{\delta f}{\tau_c}$$

$$\implies \quad \frac{p^i p^j}{ET} U^{ij} f_0 (1 + \xi f_0) + \frac{1}{\tau_\Omega} \omega^{ij} p^j \frac{\partial \delta f}{\partial p^i} = -\frac{\delta f}{\tau_c} \ , \tag{A1}$$

where, $\tau_\Omega \equiv 1/2\Omega$ and $\epsilon^{ijk} \omega^k \equiv \omega^{ij}$. In terms of the unknown constants C_n we make the following guess for δf:

$$\delta f = \sum_{n=0}^{6} C_n C_n^{kl} p^k p^l \ . \tag{A2}$$

where the fluid field gradients C_n^{ij} are given by [68],

$$\begin{aligned}
C_0^{ij} &= (3\omega^i \omega^j - \delta^{ij})(\omega^k \omega^l U^{kl} - \frac{1}{3}\vec{\nabla} \cdot \vec{u}) \ , \\
C_1^{ij} &= 2U^{ij} + \delta^{ij} U^{kl} \omega^k \omega^l - 2U^{ik} \omega^j \omega^k - 2U^{jk} \omega^k \omega^i + (\omega^i \omega^j - \delta^{ij}) \vec{\nabla} \cdot \vec{u} + \omega^i \omega^j \omega^k \omega^l U^{kl} \ , \\
C_2^{ij} &= 2(U^{ik} \omega^j \omega^k + U^{jk} \omega^i \omega^k - 2U^{kl} \omega^i \omega^j \omega^k \omega^l) \ , \\
C_3^{ij} &= U^{ik} \omega^{jk} + U^{jk} \omega^{ik} - U^{kl} \omega^{ik} \omega^j \omega^l - U^{kl} \omega^{jk} \omega^i \omega^l, \\
C_4^{ij} &= 2(U^{kl} \omega^{ik} \omega^j \omega^l + U^{kl} \omega^{jk} \omega^i \omega^l) \ , \\
C_5^{ij} &= \delta^{ij} (\vec{\nabla} \cdot \vec{u}) \ , \\
C_6^{ij} &= \delta^{ij} \omega^k \omega^l U^{kl} + \omega^i \omega^j (\vec{\nabla} \cdot \vec{u}) \ .
\end{aligned} \tag{A3}$$

Now, we calculate the required derivative of δf and substitute them in the Eq. (A1) to solve for C_n,

$$\begin{aligned}
\frac{\partial \delta f}{\partial p^i} &= \frac{\partial}{\partial p_i} \sum_{n=0}^{6} C_n C_n^{kl} p^k p^l \\
&= \sum_{n=0}^{6} C_n^{kl} p^k p^l \frac{\partial C_n}{\partial p^i} + \sum_{n=o}^{6} C_n^{kl} C_n \frac{\partial}{\partial p^i} p^k p^l.
\end{aligned}$$

It can easily be seen that the C_n for which Eq. (A1) is satisfied are functions of f^0, i.e., $C_n = C_n(f^0)$.

$$\frac{\partial \delta f}{\partial p^i} = -\frac{1}{T} f^0 (1 + \xi f^0) \sum_{n=0}^{6} \frac{dC_n}{df^0} C_n^{kl} \frac{p^k p^l p^i}{E} + \sum_{n=0}^{6} 2C_n C_n^{ik} p^k \tag{A4}$$

Using the result of Eq. (A4) in Eq. (A1) we have:

$$\frac{p^i p^j}{ET} U^{ij} f^0 (1 + \xi f^0) - \frac{1}{\tau_\Omega T} f0 (1 + \xi f^0) \sum_{n=0}^{6} \frac{dC_n}{df^0} \omega^{ij} \frac{p^i p^j p^k p^l}{E} + \frac{2}{\tau_\Omega} \sum_{n=0}^{6} C_n C_n^{ik} \omega^{ij} p^j p^k = -\frac{1}{\tau_c} \sum_{n=0}^{6} C_n C_n^{kl} p^k p^l$$

$$\implies \quad \frac{p^i p^j}{ET} U^{ij} f^0 (1 + \xi f^0) + \frac{2}{\tau_\Omega} \sum_{n=0}^{6} C_n C_n^{ik} \omega^{ij} p^j p^k = -\frac{1}{\tau_c} \sum_{n=0}^{6} C_n C_n^{kl} p^k p^l, (\text{ since, } \omega^{ij} p^i p^j = 0)$$

$$\implies \quad \frac{p^i p^j}{ET} U^{ij} f^0 (1 + \xi f^0) = \sum_{n=0}^{6} C_n \left(-\frac{2}{\tau_\Omega} C_n^{ik} \omega^{ij} p^j p^k - \frac{1}{\tau_c} C_n^{kl} p^k p^l \right) . \tag{A5}$$

The Eq. (A5) has to be solved for the C_n to obtain δf for the evaluation of viscosities. In the present article our aim is to obtain shear viscosities of the system therefore we will ignore C_5 and C_6 which correspond to bulk

viscosities and retain the first five C_n that correspond to shear stresses in the fluid. By equating the coefficients of $p^i p^j U^{ij}, U^{ij} p^j p^k \omega^{ik}, U^{ij} p^k \omega^j \omega^{ik} (\vec{p} \cdot \vec{\Omega})$ and $U^{ij} p^i \omega^j (\vec{p} \cdot \vec{\Omega})$ in Eq. (A5) to zero, we have,

$$p^i p^j U^{ij} \; : \; -\frac{4C_3}{\tau_\Omega} - \frac{2C_1}{\tau_c} = \frac{1}{ET} f^0 (1 + \xi f^0) \; ,$$

$$U^{ij} p^j p^k \omega^{ik} \; : \; -\frac{4C_1}{\tau_\Omega} + \frac{2C_3}{\tau_c} = 0 \; ,$$

$$U^{ij} p^k \omega^j \omega^{ik} (\vec{p} \cdot \vec{\Omega}) \; : \; \frac{4C_1}{\tau_\Omega} - \frac{4C_2}{\tau_\Omega} - \frac{2C_3}{\tau_c} + \frac{4C_4}{\tau_c} = 0 \; ,$$

$$U^{ij} p^i \omega^j (\vec{p} \cdot \vec{\Omega}) \; : \; \frac{8C_3}{\tau_\Omega} - \frac{4C_4}{\tau_\Omega} + \frac{4C_1}{\tau_c} - \frac{4C_2}{\tau_c} = 0 \; . \tag{A6}$$

Solving the above set of linear equations we obtain,

$$C_1 = -\frac{1}{2ET} f^0 (1 + \xi f^0) \frac{\tau_c}{1 + 4(\tau_c/\tau_\Omega)^2} \; ,$$

$$C_2 = -\frac{1}{2ET} f^0 (1 + \xi f^0) \frac{\tau_c}{1 + (\tau_c/\tau_\Omega)^2} \; ,$$

$$C_3 = -\frac{1}{ET} f^0 (1 + \xi f^0) \frac{\tau_c(\tau_c/\tau_\Omega)}{1 + 4(\tau_c/\tau_\Omega)^2} \; ,$$

$$C_4 = -\frac{1}{2ET} f^0 (1 + \xi f^0) \frac{\tau_c(\tau_c/\tau_\Omega)}{1 + 4(\tau_c/\tau_\Omega)^2} \; . \tag{A7}$$

[1] E. Shuryak, Why does the quark gluon plasma at RHIC behave as a nearly ideal fluid?, Prog. Part. Nucl. Phys. **53**, 273 (2004), arXiv:hep-ph/0312227.
[2] U. W. Heinz, Concepts of heavy ion physics, in 2nd CERN-CLAF School of High Energy Physics (2004) pp. 165–238, arXiv:hep-ph/0407360.
[3] J. Casalderrey-Solana and C. A. Salgado, Introductory lectures on jet quenching in heavy ion collisions, Acta Phys. Polon. B **38**, 3731 (2007), arXiv:0712.3443 [hep-ph].
[4] U. Heinz and R. Snellings, Collective flow and viscosity in relativistic heavy-ion collisions, Ann. Rev. Nucl. Part. Sci. **63**, 123 (2013), arXiv:1301.2826 [nucl-th].
[5] A. Beraudo et al., Extraction of Heavy-Flavor Transport Coefficients in QCD Matter, Nucl. Phys. A **979**, 21 (2018), arXiv:1803.03824 [nucl-th].
[6] L. Adamczyk et al. (STAR), Global Λ hyperon polarization in nuclear collisions: evidence for the most vortical fluid, Nature **548**, 62 (2017), arXiv:1701.06657 [nucl-ex].
[7] Z.-T. Liang and X.-N. Wang, Globally polarized quark-gluon plasma in non-central A+A collisions, Phys. Rev. Lett. **94**, 102301 (2005), [Erratum: Phys.Rev.Lett. 96, 039901 (2006)], arXiv:nucl-th/0410079.
[8] F. Becattini, F. Piccinini, and J. Rizzo, Angular momentum conservation in heavy ion collisions at very high energy, Phys. Rev. C **77**, 024906 (2008), arXiv:0711.1253 [nucl-th].
[9] I. Karpenko, Vorticity and polarization in heavy-ion collisions: Hydrodynamic models, in Strongly Interacting Matter under Rotation, edited by F. Becattini, J. Liao, and M. Lisa (Springer International Publishing, Cham, 2021) pp. 247–280.
[10] H.-L. Chen, X.-G. Huang, and J. Liao, Qcd phase structure under rotation, in Strongly Interacting Matter under Rotation, edited by F. Becattini, J. Liao, and M. Lisa (Springer International Publishing, Cham, 2021) pp. 349–379.
[11] K. Fukushima, Extreme matter in electromagnetic fields and rotation, Prog. Part. Nucl. Phys. **107**, 167 (2019), arXiv:1812.08886 [hep-ph].
[12] J. R. Letaw and J. D. Pfautsch, Quantized scalar field in rotating coordinates, Phys. Rev. D **22**, 1345 (1980).
[13] A. Vilenkin, Quantum field theory at finite temperature in a rotating system, Phys. Rev. D **21**, 2260 (1980).
[14] B. R. Iyer, DIRAC FIELD THEORY IN ROTATING COORDINATES, Phys. Rev. D **26**, 1900 (1982).
[15] G. Duffy and A. C. Ottewill, The Rotating quantum thermal distribution, Phys. Rev. D **67**, 044002 (2003), arXiv:hep-th/0211096.
[16] V. E. Ambruş and E. Winstanley, Rotating quantum states, Phys. Lett. B **734**, 296 (2014), arXiv:1401.6388 [hep-th].
[17] V. E. Ambrus and E. Winstanley, Rotating fermions inside a cylindrical boundary, Phys. Rev. D **93**, 104014 (2016), arXiv:1512.05239 [hep-th].
[18] H.-L. Chen, K. Fukushima, X.-G. Huang, and K. Mameda, Analogy between rotation and density for Dirac fermions in a magnetic field, Phys. Rev. D **93**, 104052 (2016), arXiv:1512.08974 [hep-ph].
[19] K. Mameda and A. Yamamoto, Magnetism and rotation in relativistic field theory, PTEP **2016**, 093B05 (2016), arXiv:1504.05826 [hep-th].

[20] Y. Jiang and J. Liao, Pairing Phase Transitions of Matter under Rotation, Phys. Rev. Lett. **117**, 192302 (2016), arXiv:1606.03808 [hep-ph].

[21] S. Ebihara, K. Fukushima, and K. Mameda, Boundary effects and gapped dispersion in rotating fermionic matter, Phys. Lett. B **764**, 94 (2017), arXiv:1608.00336 [hep-ph].

[22] M. N. Chernodub and S. Gongyo, Interacting fermions in rotation: chiral symmetry restoration, moment of inertia and thermodynamics, Journal of High Energy Physics **2017**, 10.1007/jhep01(2017)136 (2017).

[23] M. N. Chernodub and S. Gongyo, Effects of rotation and boundaries on chiral symmetry breaking of relativistic fermions, Phys. Rev. D **95**, 096006 (2017), arXiv:1702.08266 [hep-th].

[24] M. N. Chernodub and S. Gongyo, Edge states and thermodynamics of rotating relativistic fermions under magnetic field, Phys. Rev. D **96**, 096014 (2017), arXiv:1706.08448 [hep-th].

[25] M. N. Chernodub, Inhomogeneous confining-deconfining phases in rotating plasmas, Phys. Rev. D **103**, 054027 (2021), arXiv:2012.04924 [hep-ph].

[26] X. Wang, M. Wei, Z. Li, and M. Huang, Quark matter under rotation in the NJL model with vector interaction, Phys. Rev. D **99**, 016018 (2019), arXiv:1808.01931 [hep-ph].

[27] Y. J. (Minghua Wei and M. Huang, Mass splitting of vector mesons and spontaneous spin polarization under rotation *, Chin. Phys. C **46**, 024102 (2022), arXiv:2011.10987 [hep-ph].

[28] F. Sun and A. Huang, Properties of strange quark matter under strong rotation, Phys. Rev. D **106**, 076007 (2022), arXiv:2104.14382 [hep-ph].

[29] K. Xu, F. Lin, A. Huang, and M. Huang, $\Lambda/\bar{\Lambda}$ polarization and splitting induced by rotation and magnetic field, Phys. Rev. D **106**, L071502 (2022), arXiv:2205.02420 [hep-ph].

[30] F. Sun, K. Xu, and M. Huang, Splitting of chiral and deconfinement phase transitions induced by rotation, Phys. Rev. D **108**, 096007 (2023), arXiv:2307.14402 [hep-ph].

[31] Y. Fujimoto, K. Fukushima, and Y. Hidaka, Deconfining Phase Boundary of Rapidly Rotating Hot and Dense Matter and Analysis of Moment of Inertia, Phys. Lett. B **816**, 136184 (2021), arXiv:2101.09173 [hep-ph].

[32] F. Becattini, I. Karpenko, M. Lisa, I. Upsal, and S. Voloshin, Global hyperon polarization at local thermodynamic equilibrium with vorticity, magnetic field and feed-down, Phys. Rev. C **95**, 054902 (2017), arXiv:1610.02506 [nucl-th].

[33] S. Acharya et al. (ALICE), Global polarization of $\Lambda\bar{\Lambda}$ hyperons in Pb-Pb collisions at $\sqrt{s_{NN}} = 2.76$ and 5.02 TeV, Phys. Rev. C **101**, 044611 (2020), [Erratum: Phys.Rev.C 105, 029902 (2022)], arXiv:1909.01281 [nucl-ex].

[34] S. Acharya et al. (ALICE), Evidence of Spin-Orbital Angular Momentum Interactions in Relativistic Heavy-Ion Collisions, Phys. Rev. Lett. **125**, 012301 (2020), arXiv:1910.14408 [nucl-ex].

[35] M. S. Abdallah et al. (STAR), Pattern of global spin alignment of ϕ and K^{*0} mesons in heavy-ion collisions, Nature **614**, 244 (2023), arXiv:2204.02302 [hep-ph].

[36] G. P. Kadam and H. Mishra, Bulk and shear viscosities of hot and dense hadron gas, Nucl. Phys. A **934**, 133 (2014), arXiv:1408.6329 [hep-ph].

[37] M. I. Gorenstein, M. Hauer, and O. N. Moroz, Viscosity in the excluded volume hadron gas model, Phys. Rev. C **77**, 024911 (2008), arXiv:0708.0137 [nucl-th].

[38] K. Itakura, O. Morimatsu, and H. Otomo, Shear viscosity of a hadronic gas mixture, Phys. Rev. D **77**, 014014 (2008), arXiv:0711.1034 [hep-ph].

[39] D. Fernandez-Fraile and A. Gomez Nicola, Transport coefficients and resonances for a meson gas in Chiral Perturbation Theory, Eur. Phys. J. C **62**, 37 (2009), arXiv:0902.4829 [hep-ph].

[40] S. Plumari, A. Puglisi, F. Scardina, and V. Greco, Shear Viscosity of a strongly interacting system: Green-Kubo vs. Chapman-Enskog and Relaxation Time Approximation, Phys. Rev. C **86**, 054902 (2012), arXiv:1208.0481 [nucl-th].

[41] R. Lang, N. Kaiser, and W. Weise, Shear Viscosity of a Hot Pion Gas, Eur. Phys. J. A **48**, 109 (2012), arXiv:1205.6648 [hep-ph].

[42] J. Noronha-Hostler, J. Noronha, and C. Greiner, Transport Coefficients of Hadronic Matter near T(c), Phys. Rev. Lett. **103**, 172302 (2009), arXiv:0811.1571 [nucl-th].

[43] A. Puglisi, S. Plumari, and V. Greco, Shear viscosity η to electric conductivity σ_{el} ratio for the quark–gluon plasma, Phys. Lett. B **751**, 326 (2015), arXiv:1407.2559 [hep-ph].

[44] M. Greif, I. Bouras, C. Greiner, and Z. Xu, Electric conductivity of the quark-gluon plasma investigated using a perturbative QCD based parton cascade, Phys. Rev. D **90**, 094014 (2014), arXiv:1408.7049 [nucl-th].

[45] V. Ozvenchuk, J. M. Torres-Rincon, P. B. Gossiaux, L. Tolos, and J. Aichelin, D-meson propagation in hadronic matter and consequences for heavy-flavor observables in ultrarelativistic heavy-ion collisions, Phys. Rev. C **90**, 054909 (2014), arXiv:1408.4938 [hep-ph].

[46] M. He, R. J. Fries, and R. Rapp, Thermal Relaxation of Charm in Hadronic Matter, Phys. Lett. B **701**, 445 (2011), arXiv:1103.6279 [nucl-th].

[47] L. Tolos and J. M. Torres-Rincon, D-meson propagation in hot dense matter, Phys. Rev. D **88**, 074019 (2013), arXiv:1306.5426 [hep-ph].

[48] D. Banerjee, S. Datta, R. Gavai, and P. Majumdar, Heavy Quark Momentum Diffusion Coefficient from Lattice QCD, Phys. Rev. D **85**, 014510 (2012), arXiv:1109.5738 [hep-lat].

[49] K. Goswami, K. K. Pradhan, D. Sahu, and R. Sahoo, Diffusion and fluctuations of open charmed hadrons in an interacting hadronic medium, Phys. Rev. D **108**, 074011 (2023), arXiv:2307.04396 [hep-ph].

[50] J. M. Torres-Rincon, G. Montaña, A. Ramos, and L. Tolos, In-medium kinetic theory of D mesons and heavy-flavor transport coefficients, Phys. Rev. C **105**, 025203 (2022), arXiv:2106.01156 [hep-ph].

[51] S. Shi, J. Liao, and M. Gyulassy, Global constraints from RHIC and LHC on transport properties of QCD fluids in CUJET/CIBJET framework, Chin. Phys. C **43**, 044101 (2019), arXiv:1808.05461 [hep-ph].

[52] O. Soloveva, D. Fuseau, J. Aichelin, and E. Bratkovskaya, Shear viscosity and electric conductivity of a hot and dense QGP with a chiral phase transition, Phys. Rev. C **103**, 054901 (2021), arXiv:2011.03505 [nucl-th].

[53] R. Marty, E. Bratkovskaya, W. Cassing, J. Aichelin, and H. Berrehrah, Transport coefficients from the Nambu-Jona-Lasinio model for $SU(3)_f$, Phys. Rev. C **88**, 045204 (2013), arXiv:1305.7180 [hep-ph].

[54] S. Ghosh and S. Ghosh, One-loop Kubo estimations of the shear and bulk viscous coefficients for hot and magnetized Bosonic and Fermionic systems, Phys. Rev. D **103**, 096015 (2021), arXiv:2011.04261 [hep-ph].

[55] J. E. Bernhard, J. S. Moreland, and S. A. Bass, Bayesian estimation of the specific shear and bulk viscosity of quark–gluon plasma, Nature Phys. **15**, 1113 (2019).

[56] S. Ghosh, A. Bandyopadhyay, R. L. S. Farias, J. Dey, and G. a. Krein, Anisotropic electrical conductivity of magnetized hot quark matter, Phys. Rev. D **102**, 114015 (2020), arXiv:1911.10005 [hep-ph].

[57] J. Dey, S. Samanta, S. Ghosh, and S. Satapathy, Quantum expression for the electrical conductivity of massless quark matter and of the hadron resonance gas in the presence of a magnetic field, Phys. Rev. C **106**, 044914 (2022), arXiv:2002.04434 [nucl-th].

[58] P. Kalikotay, S. Ghosh, N. Chaudhuri, P. Roy, and S. Sarkar, Medium effects on the electrical and Hall conductivities of a hot and magnetized pion gas, Phys. Rev. D **102**, 076007 (2020), arXiv:2009.10493 [hep-ph].

[59] J. Dey, A. Bandyopadhyay, A. Gupta, N. Pujari, and S. Ghosh, Electrical conductivity of strongly magnetized dense quark matter - possibility of quantum Hall effect, Nucl. Phys. A **1034**, 122654 (2023), arXiv:2103.15364 [hep-ph].

[60] S. Satapathy, S. Ghosh, and S. Ghosh, Kubo estimation of the electrical conductivity for a hot relativistic fluid in the presence of a magnetic field, Phys. Rev. D **104**, 056030 (2021), arXiv:2104.03917 [hep-ph].

[61] A. Das, H. Mishra, and R. K. Mohapatra, Electrical conductivity and Hall conductivity of a hot and dense hadron gas in a magnetic field: A relaxation time approach, Phys. Rev. D **99**, 094031 (2019), arXiv:1903.03938 [hep-ph].

[62] A. Das, H. Mishra, and R. K. Mohapatra, Electrical conductivity and Hall conductivity of a hot and dense quark gluon plasma in a magnetic field: A quasiparticle approach, Phys. Rev. D **101**, 034027 (2020), arXiv:1907.05298 [hep-ph].

[63] B. Chatterjee, R. Rath, G. Sarwar, and R. Sahoo, Centrality dependence of Electrical and Hall conductivity at RHIC and LHC energies for a Conformal System, Eur. Phys. J. A **57**, 45 (2021), arXiv:1908.01121 [hep-ph].

[64] K. Hattori and D. Satow, Electrical Conductivity of Quark-Gluon Plasma in Strong Magnetic Fields, Phys. Rev. D **94**, 114032 (2016), arXiv:1610.06818 [hep-ph].

[65] K. Hattori, S. Li, D. Satow, and H.-U. Yee, Longitudinal Conductivity in Strong Magnetic Field in Perturbative QCD: Complete Leading Order, Phys. Rev. D **95**, 076008 (2017), arXiv:1610.06839 [hep-ph].

[66] S. Satapathy, S. Ghosh, and S. Ghosh, Quantum field theoretical structure of electrical conductivity of cold and dense fermionic matter in the presence of a magnetic field, Phys. Rev. D **106**, 036006 (2022), arXiv:2112.08236 [hep-ph].

[67] A. Dwibedi, C. W. Aung, J. Dey, and S. Ghosh, Effect of the Coriolis force on the electrical conductivity of quark matter: A nonrelativistic description, Phys. Rev. C **109**, 034914 (2024), arXiv:2305.10183 [nucl-th].

[68] C. W. Aung, A. Dwibedi, J. Dey, and S. Ghosh, Effect of Coriolis force on the shear viscosity of quark matter: A nonrelativistic description, Phys. Rev. C **109**, 034913 (2024), arXiv:2303.16462 [nucl-th].

[69] N. Padhan, A. Dwibedi, A. Chatterjee, and S. Ghosh, Effect of Coriolis force on electrical conductivity tensor for the rotating hadron resonance gas, Phys. Rev. C **110**, 024904 (2024), arXiv:2403.16647 [hep-ph].

[70] N. Padhan, A. Dwibedi, D. Das, A. Chatterjee, S. De, and S. Ghosh, Effect of Coriolis Force on Diffusion of D Meson, (2024), arXiv:2411.09983 [hep-ph].

[71] J. I. Kapusta, E. Rrapaj, and S. Rudaz, Relaxation Time for Strange Quark Spin in Rotating Quark-Gluon Plasma, Phys. Rev. C **101**, 024907 (2020), arXiv:1907.10750 [nucl-th].

[72] C. Misner, K. Thorne, J. Wheeler, and D. Kaiser, Gravitation (Princeton University Press, 2017).

[73] B. Schutz, A First Course in General Relativity (Cambridge University Press, 2009).

[74] C. Cercignani and G. M. Kremer, Riemann spaces and general relativity, in The Relativistic Boltzmann Equation: Theory and Applications (Birkhäuser Basel, Basel, 2002) pp. 291–325.

[75] G. M. Kremer, Relativistic gas in a Schwarzschild metric, J. Stat. Mech. **1304**, P04016 (2013), [Erratum: J.Stat.Mech. 1305, E05001 (2013)], arXiv:1212.5573 [gr-qc].

[76] C. Cercignani and G. M. Kremer, Boltzmann equation in gravitational fields, in The Relativistic Boltzmann Equation: Theory and Applications (Birkhäuser Basel, Basel, 2002) pp. 327–346.

[77] F. Debbasch and W. van Leeuwen, General relativistic boltzmann equation, i: Covariant treatment, Physica A: Statistical Mechanics and its Applications **388**, 1079 (2009).

[78] F. Debbasch and W. van Leeuwen, General relativistic boltzmann equation, ii: Manifestly covariant treatment, Physica A: Statistical Mechanics and its Applications **388**, 1818 (2009).

[79] P. Romatschke, Relativistic (Lattice) Boltzmann Equation with Non-Ideal Equation of State, Phys. Rev. D **85**, 065012 (2012), arXiv:1108.5561 [gr-qc].

[80] J. Dey, S. Satapathy, P. Murmu, and S. Ghosh, Shear viscosity and electrical conductivity of the relativistic fluid in the presence of a magnetic field: A massless case, Pramana **95**, 125 (2021), arXiv:1907.11164 [hep-ph].

[81] F. Karsch and K. Redlich, Probing freeze-out conditions in heavy ion collisions with moments of charge fluctuations, Physics Letters B **695**, 136 (2011).

[82] P. Garg, D. Mishra, P. Netrakanti, B. Mohanty, A. Mohanty, B. Singh, and N. Xu, Conserved number fluctuations in a hadron resonance gas model, Physics Letters B **726**, 691 (2013).

[83] V. Vovchenko, D. V. Anchishkin, M. I. Gorenstein, and R. V. Poberezhnyuk, Scaled variance, skewness, and kurtosis near the critical point of nuclear matter, Phys. Rev. C **92**, 054901 (2015).

[84] O. Savchuk, V. Vovchenko, R. V. Poberezhnyuk, M. I. Gorenstein, and H. Stoecker, Traces of the nuclear liquid-gas phase transition in the analytic properties of hot qcd, Phys. Rev. C **101**, 035205 (2020).

[85] D. K. Mishra, P. Garg, P. K. Netrakanti, and A. K. Mohanty, Effect of resonance decay on conserved number fluctuations in a hadron resonance gas model, Phys. Rev. C **94**, 014905 (2016).

[86] M. Albright, J. Kapusta, and C. Young, Matching excluded-volume hadron-resonance gas models and perturbative qcd to lattice calculations, Phys. Rev. C **90**, 024915 (2014).

[87] F. Karsch, K. Redlich, and A. Tawfik, Thermodynamics at nonzero baryon number density: A Comparison of lattice and hadron resonance gas model calculations, Phys. Lett. B **571**, 67 (2003), arXiv:hep-ph/0306208.

[88] P. Braun-Munzinger, V. Koch, T. Schäfer, and J. Stachel, Properties of hot and dense matter from relativistic heavy ion collisions, Phys. Rept. **621**, 76 (2016), arXiv:1510.00442 [nucl-th].

[89] V. V. Begun, M. I. Gorenstein, M. Hauer, V. P. Konchakovski, and O. S. Zozulya, Multiplicity Fluctuations in Hadron-Resonance Gas, Phys. Rev. C **74**, 044903 (2006), arXiv:nucl-th/0606036.

[90] M. Nahrgang, M. Bluhm, P. Alba, R. Bellwied, and C. Ratti, Impact of resonance regeneration and decay on the net-proton fluctuations in a hadron resonance gas, Eur. Phys. J. C **75**, 573 (2015), arXiv:1402.1238 [hep-ph].

[91] A. Bazavov et al. (HotQCD), Fluctuations and Correlations of net baryon number, electric charge, and strangeness: A comparison of lattice QCD results with the hadron resonance gas model, Phys. Rev. D **86**, 034509 (2012), arXiv:1203.0784 [hep-lat].

[92] A. Bhattacharyya, S. Das, S. K. Ghosh, R. Ray, and S. Samanta, Fluctuations and correlations of conserved charges in an excluded volume hadron resonance gas model, Phys. Rev. C **90**, 034909 (2014), arXiv:1310.2793 [hep-ph].

[93] A. Chatterjee, S. Chatterjee, T. K. Nayak, and N. R. Sahoo, Diagonal and off-diagonal susceptibilities of conserved quantities in relativistic heavy-ion collisions, J. Phys. G **43**, 125103 (2016), arXiv:1606.09573 [nucl-ex].

[94] J. Noronha-Hostler, J. Noronha, and C. Greiner, Hadron Mass Spectrum and the Shear Viscosity to Entropy Density Ratio of Hot Hadronic Matter, Phys. Rev. C **86**, 024913 (2012), arXiv:1206.5138 [nucl-th].

[95] S. K. Tiwari, P. K. Srivastava, and C. P. Singh, Description of Hot and Dense Hadron Gas Properties in a New Excluded-Volume model, Phys. Rev. C **85**, 014908 (2012), arXiv:1111.2406 [hep-ph].

[96] K. K. Pradhan, D. Sahu, R. Scaria, and R. Sahoo, Conductivity, diffusivity, and violation of the Wiedemann-Franz Law in a hadron resonance gas with van der Waals interactions, Phys. Rev. C **107**, 014910 (2023), arXiv:2205.03149 [hep-ph].

[97] H.-X. Zhang, J.-W. Kang, and B.-W. Zhang, In-medium effect on the thermodynamics and transport coefficients in the van der Waals hadron resonance gas, Phys. Rev. D **101**, 114033 (2020), arXiv:1905.08146 [hep-ph].

[98] S. Samanta, S. Ghosh, and B. Mohanty, Finite size effect of hadronic matter on its transport coefficients, J. Phys. G **45**, 075101 (2018), arXiv:1706.07709 [hep-ph].

[99] S. Ghosh, S. Samanta, S. Ghosh, and H. Mishra, Viscosity calculations from Hadron Resonance Gas model: Finite size effect, Int. J. Mod. Phys. E **28**, 1950036 (2019), arXiv:1906.06029 [nucl-th].

[100] S. Ghosh, S. Ghosh, and S. Bhattacharyya, Phenomenological bound on the viscosity of the hadron resonance gas, Phys. Rev. C **98**, 045202 (2018), arXiv:1807.03188 [hep-ph].

[101] G. S. Rocha and G. S. Denicol, Transport coefficients of transient hydrodynamics for the hadron-resonance gas and thermal-mass quasiparticle models, Phys. Rev. D **109**, 096011 (2024), arXiv:2402.06996 [nucl-th].

[102] R. Dashen, S.-K. Ma, and H. J. Bernstein, S Matrix formulation of statistical mechanics, Phys. Rev. **187**, 345 (1969).

[103] R. F. Dashen and R. Rajaraman, Narrow Resonances in Statistical Mechanics, Phys. Rev. D **10**, 694 (1974).

[104] C. Amsler et al. (Particle Data Group), Review of Particle Physics, Phys. Lett. B **667**, 1 (2008).

[105] C. Ratti and R. Bellwied, The hadron resonance gas model, in The Deconfinement Transition of QCD: Theory Meets Experiment (Springer International Publishing, Cham, 2021) pp. 111–131.

[106] P. Kovtun, D. T. Son, and A. O. Starinets, Viscosity in strongly interacting quantum field theories from black hole physics, Phys. Rev. Lett. **94**, 111601 (2005), arXiv:hep-th/0405231.

[107] Y. Jiang, Z.-W. Lin, and J. Liao, Rotating quark-gluon plasma in relativistic heavy ion collisions, Phys. Rev. C **94**, 044910 (2016), [Erratum: Phys.Rev.C 95, 049904 (2017)], arXiv:1602.06580 [hep-ph].

[108] K. Tuchin, On viscous flow and azimuthal anisotropy of quark-gluon plasma in strong magnetic field, J. Phys. G **39**, 025010 (2012), arXiv:1108.4394 [nucl-th].

[109] R. K. Mohapatra, P. S. Saumia, and A. M. Srivastava, Enhancement of flow anisotropies due to magnetic field in relativistic heavy-ion collisions, Mod. Phys. Lett. A **26**, 2477 (2011), arXiv:1102.3819 [hep-ph].